

## FUNNEL FLOWS FROM DISKS TO MAGNETIZED STARS

A.V. KOLDOBA<sup>1</sup>, R.V.E. LOVELACE<sup>2</sup>, G.V. USTYUGOVA<sup>3</sup>, M.M. ROMANOVA<sup>2</sup>  
Draft version November 2, 2018

## ABSTRACT

This work considers flows from an accretion disk corotating with the aligned dipole magnetic field of a rotating star. Ideal magnetohydrodynamics (MHD) is assumed with the pressure and density related as  $p \propto \rho^\gamma$  and with  $\rho \mathbf{v}^2 \ll \mathbf{B}^2/4\pi$ , where  $\mathbf{v}$  is the flow velocity. This limit corresponds to the Alfvén radius for the disk accretion larger than the corotation radius and is of particular interest because flow can be solved rigorously. Transonic flows, which go from subsonic motion near the disk to supersonic inflow near the star, are shown to be possible only for a narrow range of  $R_d \sim r_c \equiv (GM/\Omega^2)^{1/3}$ , where  $R_d$  is the radius at which the dipole field line intersects the disk,  $r_c$  the corotation radius,  $M$  the mass of the star, and  $\Omega$  its angular rotation rate. Over a larger range of  $R_d \lesssim r_c$ , subsonic flows from the disk to the star are possible. The transonic flows have very different behaviors for  $\gamma > 7/5$  and  $< 7/5$ . In both cases, the plasma flow velocity  $\mathbf{v}$  (which is parallel to  $\mathbf{B}$ ) increases with decreasing distance  $R$  from the star. However, for  $\gamma > 7/5$ , the Mach number  $\mathcal{M} \equiv |\mathbf{v}|/c_s$  (with  $c_s$  the sound speed) initially increases with  $R$  decreasing from  $R_d$ , but for  $R$  decreasing from  $\approx 0.22R_d$  (for  $\gamma = 5/3$ ) the Mach number surprisingly *decreases*. In the other limit,  $\gamma < 7/5$ ,  $\mathcal{M}$  increases monotonically with decreasing  $R$ . Application of these results is made to funnel flows to rotating magnetized neutron stars and young stellar objects. The spatial variation of *both* the flow velocity and the Mach number are crucial to the nature of the standing shock wave near the star and to the determination of emission line profiles.

*Subject headings:* physical processes: accretion, accretion disks: hydrodynamics: plasmas — stars: formation: magnetic fields: pulsars

## 1. INTRODUCTION

Models of magnetohydrodynamic (MHD) disk accretion to a rotating star with an aligned dipole magnetic field have been discussed by many authors (e.g., Ghosh & Lamb 1979; Camenzind 1990; Königl 1991; Lovelace, Romanova, & Bisnovatyi-Kogan 1995). Major uncertainties remain however because of the many assumptions required to solve the MHD equations. For example, the validity of the standard formula for the disk’s Alfvén radius (Shapiro & Teukolsky 1983) is unknown and in fact this radius may depend on the rotation rate of the star (Lovelace, Romanova, & Bisnovatyi-Kogan 1999).

Definite predictions can be made about funnel flows from disks to magnetized stars assuming a dipole magnetic field. These flows shown in Figure 1 naturally explain the large infall velocities observed in many T Tauri stars (Hartmann, Hewett, & Calvet 1994; Martin 1996; Najita *et al.* 2000). Such flows may also occur in disk accretion to rotating magnetized neutron stars (Li & Wilson 1999). Here, a study is made of stationary, axisymmetric ideal magnetohydrodynamic (MHD) flows from an accretion disk to a rotating star with an aligned dipole magnetic field. The MHD equations lead to a Bernoulli equation which we analyze in the general case where pressure and density of a fluid particle are related as  $p \propto \rho^\gamma$  at constant entropy. A Bernoulli equation for the isothermal case  $p \propto \rho$  was discussed earlier by Li and Wilson (1999). Detailed calculations of emission line shapes were made by Hartmann *et al.* (1994) and Martin (1996) for a model where plasma free-falls along dipole field lines of

an aligned rotator, but these authors do not analyze the Bernoulli equation and do not consider the sonic point of the flow.

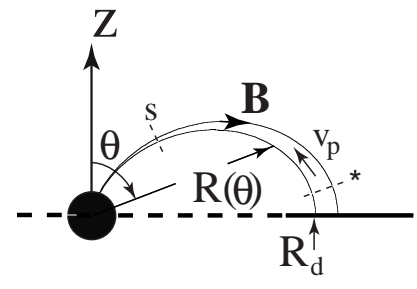


FIG. 1.— The figure shows a plasma accretion disk corotating with the aligned magnetic dipole field of a star. Plasma flows from the disk to the star along a flux tube of the dipole, going from subsonic to supersonic flow. Conservation of magnetic flux gives  $B_p A_p = \text{const}$ , and conservation of mass gives  $\rho v_p A_p = \text{const}$ , where  $v_p$  is the plasma speed along the field line and  $A_p$  is the cross sectional area of the flux tube. The dashed line marked with (\*) indicates the sonic point and that marked with (s) indicates a standing shock.

We use inertial, cylindrical  $(r, \phi, z)$  and spherical  $(R, \theta, \phi)$  coordinate systems. As in the case of matter outflow along open magnetic field lines threading a disk (Ustyugova *et al.* 1999), there are a number of integrals of the plasma motion which are conserved along magnetic field lines labeled by the flux function  $\Psi(r, z) = rA_\phi = \text{const}$ , where  $A_\phi$  is the vector potential. The constant  $K(\Psi)$  arises from the conservation of mass,  $\Omega(\Psi)$  from conservation of helicity,  $\Lambda(\Psi)$  from conservation of

<sup>1</sup> Institute of Mathematical Modelling, Russian Academy of Sciences, Moscow, Russia, 125047

<sup>1</sup> Department of Astronomy, Cornell University, Ithaca, NY 14853-6801; rvl1@cornell.edu; romanova@astrosun.tn.cornell.edu

<sup>3</sup> Keldysh Institute of Applied Mathematics, Russian Academy of Sciences, Moscow, Russia, 125047, ustyugg@spp.Keldysh.ru

angular momentum,  $S(\Psi)$  from conservation of specific entropy, and  $E(\Psi)$  from conservation of energy (Bernoulli's constant) (see for example Ustyugova *et al.* 1999).

$$\mathbf{v}_p = \frac{K(\Psi)}{4\pi\rho} \mathbf{B}_p, \quad \Omega(\Psi) = \omega - \frac{KB_\phi}{4\pi\rho r}, \quad (1)$$

$$\Lambda(\Psi) = \omega r^2 - \frac{rB_\phi}{K}, \quad S = S(\Psi), \quad (2)$$

$$E(\Psi) = \frac{v_p^2}{2} + \frac{1}{2}(\omega - \Omega)^2 r^2 + w + \Phi_g - \frac{\Omega^2 r^2}{2}, \quad (3)$$

where the  $p$  subscript indicates the poloidal  $(r, z)$  [or  $(R, \theta)$ ] part of the vector,  $\omega = v_\phi/r$  the angular velocity of the matter,  $w$  is the specific enthalpy, and  $\Phi_g = -GM/R$  the gravitational potential of the star. (The mass of the disk is assumed negligible.) An additional equation - the Grad-Shafranov equation - follows from the equilibrium of forces across magnetic field lines (Lovelace *et al.* 1986).

In §2 we discuss simplifications which occur in the strong field limit, and in §3 we analyze the Bernoulli equation (3). In §4 dimensionless variables are introduced. In §5 we discuss the nature of the transonic solutions which go from subsonic flow near the disk to supersonic flow near the star and show that the behavior of the flows is different for  $\gamma < 7/5$  and  $\gamma > 7/5$ . In §6, we describe the nature of the possible subsonic outflows from the disk to the star. In §7, we contrast the considered flows with spherical Bondi accretion. In §8 we discuss conditions for the strong field approximation to hold. In §9 we apply the theory to accretion to a neutron star and to a young stellar object. In §10 we summarize the work.

## 2. STRONG FIELD APPROXIMATION

We investigate the case where the magnetic field of the star is dominant. Namely, we suppose that the star has dipole magnetic moment  $\boldsymbol{\mu}$  in the direction coinciding with rotation axis of the disk. Thus the poloidal magnetic field in the considered region is the dipole magnetic,  $\mathbf{B}_p = 3\mathbf{R}(\boldsymbol{\mu} \cdot \mathbf{R})/R^5 - \boldsymbol{\mu}/R^3$ . Further, we suppose that the magnetic field energy-density is dominant compared with matter energy-density,

$$\frac{B_p^2}{8\pi} \gg (p, \rho v^2, \rho\Phi). \quad (4)$$

Hence the matter flow does not disturb the dipole magnetic field significantly, and the toroidal component of the magnetic field is small,  $|B_\phi| \ll |\mathbf{B}_p|$ . Consequently, the full Grad-Shafranov equation is not needed. In §8 we give necessary conditions for the strong field approximation to hold.

In spherical coordinates, the flux function of the dipole magnetic field is  $\Psi = \mu \sin^2(\theta)/R$ . Thus, the equation for the dipole field lines is

$$R = R_d(\Psi) \sin^2 \theta, \quad (5)$$

where  $R_d(\Psi) = \mu/\Psi$  is the radius at which the magnetic field line  $\Psi = \text{const}$  passes through the disk ( $z = 0$ ). Note that  $B_R = (R^2 \sin \theta)^{-1} \partial \Psi / \partial \theta = 2\mu \cos \theta / R^3$ , and  $B_\theta = -(R \sin \theta)^{-1} \partial \Psi / \partial R = \mu \sin \theta / R^3$ . Figure 1 shows the envisioned geometry.

Equations (1) and (2) can be solved for  $\omega$  and  $B_\phi$  to give

$$\omega = \Omega \frac{1 - (\rho_A/\rho)(h/r^2)}{1 - \rho_A/\rho}, \quad B_\phi = r\Omega \sqrt{4\pi\rho_A} \frac{1 - h/r^2}{1 - \rho_A/\rho}, \quad (6)$$

where  $\rho_A \equiv K^2/(4\pi)$  and  $h \equiv \Lambda/\Omega$ . Note that  $\rho_A/\rho = v_p^2/v_{Ap}^2$  is the poloidal Alfvén Mach number squared calculated using the Alfvén velocity  $v_{Ap} \equiv |\mathbf{B}_p|/\sqrt{4\pi\rho}$ . Owing to our assumptions,  $\rho_A/\rho \ll 1$  everywhere in the considered region. Consequently,

$$\omega - \Omega = \Omega \frac{\rho_A}{\rho} \left(1 - \frac{h}{r^2}\right), \quad B_\phi = \Omega r \sqrt{4\pi\rho_A} \left(1 - \frac{h}{r^2}\right). \quad (7)$$

We assume further that  $(\rho_A/\rho)|1 - h/r^2| \ll 1$  with the result that  $|\omega - \Omega| \ll \Omega$ . From equation (13) note that  $|B_\phi|/|\mathbf{B}_p| = (r\Omega/v_{Ap})|1 - h/r^2| \ll 1$ .

Thus a given fluid particle moves along the poloidal magnetic field  $\mathbf{v}_p \propto \mathbf{B}_p$ , and its angular velocity  $\Omega(\Psi)$  is a constant. The value  $\Omega(\Psi)$  is the angular velocity of rotation of the footpoint of the magnetic field line  $\Psi = \text{const}$ , which we suppose is frozen into the star. Thus,  $\Omega(\Psi) = \Omega_{\text{star}} = \text{const}$  is the angular rotation rate of the star. We omit the subscript on  $\Omega$  in the following.

## 3. BERNOULLI'S CONSTANT

Consider now the matter flow along a specific magnetic field line  $R = R_d(\Psi) \sin^2 \theta$ . The effective potential along this line in a reference frame rotating with rate  $\Omega$  is

$$\Phi(R) = \Phi_g + \Phi_c = -\frac{GM}{R} - \frac{\Omega^2 R^2 \sin^2 \theta}{2} = -\frac{GM}{R} - \frac{\Omega^2 R^3}{2R_d}. \quad (8)$$

The magnitude of the magnetic field along this field line is

$$B_p(R) = \frac{\mu}{R^3} (4 - 3 \sin^2 \theta)^{1/2} = \frac{\mu}{R^3} \left(4 - \frac{3R}{R_d}\right)^{1/2}. \quad (9)$$

Thus the Bernoulli constant along this field line is

$$E = F(R, \rho) = \frac{K^2 \mu^2}{32\pi^2 \rho^2 R^6} \left(4 - \frac{3R}{R_d}\right) + w + \Phi(R), \quad (10)$$

where  $w = S\rho^{\gamma-1}/(\gamma-1) = c_s^2/(\gamma-1)$ , with  $c_s$  the sound speed and  $S \equiv \gamma p/\rho^\gamma$  the specific entropy.

We consider flows which are subsonic near the disk,  $|v_p| \ll c_s$  for  $R \lesssim R_d$ . There are then three possible cases: (1) The flow is transonic, going from subsonic to supersonic at some distances  $R_* < R_d$ ; (2) The flow remains subsonic between the disk and the star; or (3) no stationary solution to the Bernoulli equation exists.

For the transonic flows, note that the  $\rho$  derivative of equation (10) is

$$\left. \frac{\partial F}{\partial \rho} \right|_R = \frac{c_s^2 - v_p^2}{\rho}, \quad (11)$$

in that  $(\partial w / \partial \rho)_S = c_s^2/\rho$ . In general  $F(R, \rho)$  has a minimum as a function of  $\rho$  at, say,  $\rho_m(R)$ , and  $E = F(R, \rho)$  has two solutions for  $\rho$ . The larger  $\rho$  solution has  $\partial F / \partial \rho > 0$  and corresponds to subsonic flow. The smaller  $\rho$  solution has  $\partial F / \partial \rho < 0$  and corresponds to supersonic flow.

For the transonic flows, the conditions for a smooth transition through the sonic point are

$$\left. \frac{\partial F}{\partial R} \right|_* = 0, \quad \left. \frac{\partial F}{\partial \rho} \right|_* = 0. \quad (12)$$

In order to pass from subsonic to supersonic flow, this extremum of  $F(R, \rho)$  must be a saddle point which corresponds to  $F_{RR*} F_{\rho\rho*} - F_{\rho R*}^2 < 0$ , where the subscripts indicate partial derivatives. The conditions for this are given in §5.

## 4. DIMENSIONLESS VARIABLES

With  $R$  measured in units of  $R_d$ , we can write the effective potential as

$$\Phi = -\Omega^2 r_c^2 \left( \frac{\alpha}{R/R_d} + \frac{(R/R_d)^3}{2\alpha^2} \right),$$

where  $\alpha \equiv r_c/R_d$ , and the characteristic length

$$r_c \equiv \left( \frac{GM}{\Omega^2} \right)^{1/3} \approx 1.5 \times 10^8 \text{cm} \left( \frac{M}{M_\odot} \right)^{1/2} \left( \frac{P}{1\text{s}} \right)^{2/3} \quad (13)$$

is the ‘‘centrifugal radius’’ where the centrifugal force balances the gravitational attraction of the star (in the  $z = 0$  plane in the absence of magnetic forces), and  $P = 2\pi/\Omega$  is the star’s rotation period. For a young star of solar mass,  $r_c \approx 2.9 \times 10^{11} \text{cm} (P/1\text{d})^{2/3}$ .

Useful dimensionless variables are

$$\begin{aligned} \hat{R} &= \frac{R}{R_d}, & \hat{\rho} &= \frac{4\pi\alpha\Omega R_d^4}{K\mu} \rho, \\ \hat{E} &= \frac{E}{\Omega^2 r_c^2}, & \hat{S} &= \frac{S}{\Omega^2 r_c^2} \left( \frac{K\mu}{4\pi\alpha\Omega R_d^4} \right)^{\gamma-1}, \end{aligned} \quad (14)$$

and  $\hat{F} = F/(\Omega r_c)^2$ ,  $(\hat{c}_s)^2 = \hat{S}\hat{\rho}^{\gamma-1} = c_s^2/(\Omega r_c)^2$ ,  $\hat{v}_p = v_p/(\Omega r_c) = (4 - 3\hat{R})^{1/2}/(\hat{\rho}\hat{R}^3)$ , where  $\alpha = r_c/R_d$ . Note that at  $\hat{R} = 1$ ,  $\hat{\rho}\hat{v}_p = 1$ . For simplicity of notation we now drop the hats. We then have  $R_{star}/R_d < R \leq 1$ , where  $R_{star}$  is the star’s radius.

In terms of these variables, Bernoulli’s equation becomes

$$E = F(R, \rho) = \frac{4 - 3R}{2\rho^2 R^6} + \frac{S\rho^{\gamma-1}}{\gamma - 1} - \left( \frac{\alpha}{R} + \frac{R^3}{2\alpha^2} \right). \quad (15)$$

We suppose that the disk matter is at a relatively low temperature, that is,  $w(R_d) = c_s^2(R_d)/(\gamma - 1) \ll -\Phi(R_d)$ , and that the outflow speed from the disk is small  $v_p^2(R_d) \ll -\Phi(R_d)$ . Under these conditions the dimensionless quantities at the starting point of the flow ( $R = 1$ ) are: the Bernoulli constant,  $E \approx -\alpha - 1/2\alpha^2$ , the sound speed,  $c_s(1) \ll 1$ , and the density,  $\rho(1) \gg 1$ . Because  $S = c_s^2/\rho^{\gamma-1}$ , we also have  $S = S(1) \ll 1$ .

## 5. TRANSONIC FLOWS

The mentioned conditions for a smooth transition through the sonic point give

$$0 = \left. \frac{\partial F}{\partial R} \right|_* = -\frac{3(8 - 5R_*)}{2\rho_*^2 R_*^7} + \frac{\alpha}{R_*^2} - \frac{3R_*^2}{2\alpha^2}, \quad (16)$$

$$0 = \left. \frac{\partial F}{\partial \rho} \right|_* = -\frac{4 - 3R_*}{\rho_*^3 R_*^6} + S\rho_*^{\gamma-2}. \quad (17)$$

In general,  $F_{\rho\rho} > 0$ . In order for this critical point to be a saddle point of  $F(R, \rho)$ , we must have  $F_{RR} < F_{\rho\rho}^2/F_{\rho\rho}$ . This requirement is satisfied if  $R_* > (N/D)^{1/4} (2\alpha^3/3)^{1/4}$ , where  $N = 30\gamma R_*^2 - 45R_*^2 + 140R_* - 100\gamma R_* + 80\gamma - 112$  and  $D = 60\gamma R_*^2 - 15R_*^2 + 52R_* - 188\gamma R_* + 144\gamma - 48$ . This condition on  $R_*$  is always satisfied if  $\gamma \leq 7/4$ . For  $\gamma = 5/3$ , the condition is satisfied for  $R_* > 0.581(2\alpha^3/3)^{1/4}$ . The nature of the function  $F(R, \rho)$  can be understood from its contour plot shown in Figure 2a for a sample case.

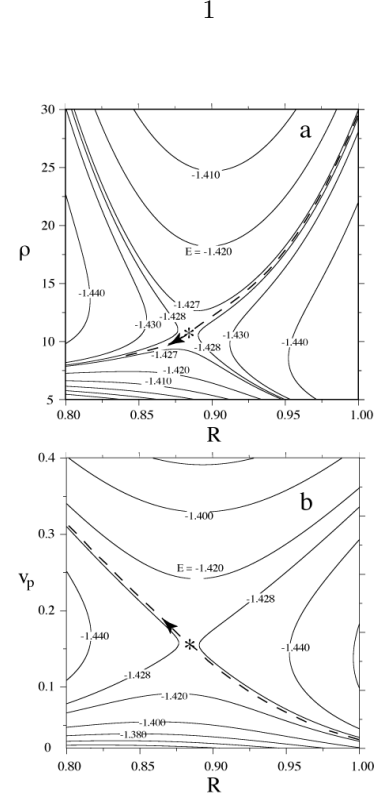


FIG. 2.— Contours of the Bernoulli function  $E = F(R, \rho)$  in the top panel (a) and  $E = F(R, v_p)$  in the bottom panel (b), for a sample case with  $\gamma = 5/3$ , dimensionless entropy  $S = 0.005$ , and  $\alpha = 1$ . Distance from the center of the star  $R$  is normalized by  $R_d$ . The transonic flow starts at  $R = 1$  and follows the dashed line. The sonic point where  $v_p = c_s$  - indicated by the asterisk - is the saddle point of the surface  $F$  at  $(R_*, \rho_*)$ . For  $R > R_*$  the flow is subsonic and  $\partial F/\partial \rho > 0$ , while for the reversed inequalities the flow is supersonic. A possible subsonic flow would follow the upper  $E = -1.42$  contour in (a) and the lower  $E = -1.42$  contour in (b).

The term in equation (16) involving  $\rho_*$  can be rewritten in terms of  $S$  using equation (17). This term is then seen to be negligible compared with the terms involving  $\alpha$  because  $S \ll 1$ . Equation (16) is then seen to correspond to a balance of the gravitational attraction and centrifugal force along the field line. Under this condition, equation (16) can be satisfied only for

$$\alpha \leq \alpha_0 \equiv (3/2)^{1/3} \approx 1.145. \quad (18)$$

Consequently,

$$\begin{aligned} R_* &\approx \left( \frac{2\alpha^3}{3} \right)^{1/4}, & \rho_* &\approx S^{-\frac{1}{\gamma+1}} \left( \frac{4 - 3R_*}{R_*^6} \right)^{\frac{1}{\gamma+1}}, \\ c_{s*} &= (S\rho_*^{\gamma-1})^{1/2} \approx S^{\frac{1}{\gamma+1}} \left( \frac{4 - 3R_*}{R_*^6} \right)^{\frac{\gamma-1}{2(\gamma+1)}}. \end{aligned} \quad (19)$$

Thus the mass flux-density is  $\rho_* v_{p*} = \rho_* c_{s*} = (4 - 3R_*)^{1/2}/R_*^3$ . The approximation involves neglecting the  $\rho_*$  term in equation (16) which is valid for  $S \ll 1$  and  $\alpha$  not too small compared with unity. In the next approximation, we find  $R_* \approx (2\alpha^3/3)^{1/4} [1 - 1.15S^{3/4}\alpha^{-11/8}]$  for  $\gamma = 5/3$ , and  $R_* \approx (2\alpha^3/3)^{1/4} [1 - 0.88S^{0.87}\alpha^{-0.84}]$  for  $\gamma = 1.3$ , and both expressions for  $R_* \ll 1$ . If the factor in the square brackets is less than about 0.863 then

as mentioned below equation (17) the saddle point disappears (by becoming a minimum). The saddle point given by equation (19) is the only saddle point with  $R_* \leq 1$ . Figure 3 shows the dependences of  $R_*$  and  $c_{s*}$  obtained by solving equations (16) and (17) numerically without approximations.

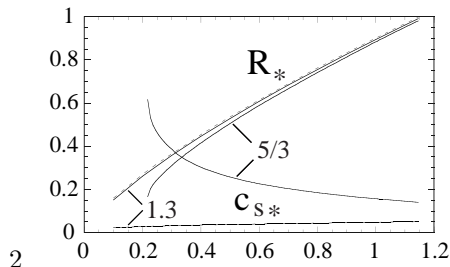


FIG. 3.— Dependences of the sonic point distance  $R_*$  and sound speed  $c_*$  on  $\alpha = r_c/R_d$  for the cases of  $\gamma = 5/3$  and  $\gamma = 1.3$  and dimensionless entropy  $S = 0.005$ . The dashed line is for the approximation of equation (19). For the  $\gamma = 5/3$  case, the saddle point of  $F(R, \rho)$  changes into a minimum for  $\alpha < 0.218$  so that these values are not of interest.

Figures (4) and (5) show sample radial profiles of the fluid variables for  $\gamma = 5/3$  and 1.3, respectively. A value of  $\gamma$  smaller than the ideal monotonic gas value is of interest for a high temperature plasmas where the electron heat conduction can be modeled by smaller  $\gamma$  (as is the case for the solar wind). The difference in behavior of the cases shown in Figures (4) and (5) can be understood by considering the Bernoulli equation for  $R \ll 1$ . In this limit  $v_p \approx (2\alpha/R)^{1/2}$  [in dimensional variables this is  $v_p \approx (2GM/R)^{1/2}$ , which is the free-fall speed],  $\rho \approx (2/\alpha)^{1/2}R^{-5/2}$ , and  $c_s \approx (2/\alpha)^{(\gamma-1)/4}S^{1/2}R^{-5(\gamma-1)/4}$ . Hence the Mach number varies as  $\mathcal{M} = v_p/c_s \approx 2(\alpha/2)^{(\gamma+1)/4}S^{-1/2}R^{(5\gamma-7)/4}$ . Thus for  $\gamma > 7/5$ , the Mach number initially increases with decreasing  $R$ , but for small enough  $R$ ,  $\mathcal{M}$  decreases with decreasing  $R$ . The radius of the maximum of  $\mathcal{M}$  is found to be  $R_{max} \approx (5\gamma - 7)/\{6(\gamma - 1)[1 + 1/(2\alpha^3)]\}$ . The maximum value of  $\mathcal{M}$  is therefore  $\propto S^{-1/2}$ . On the other hand for  $\gamma < 7/5$ ,  $\mathcal{M}$  increases monotonically with decreasing  $R$ . Therefore, the changeover in behavior between Figures (4) and (5) occurs at  $\gamma = 7/5$ . The radial variation of both  $v_p$  and  $\mathcal{M}$  are clearly important for calculations of the emission line profiles (Hartmann *et al.* 1994).

For  $\gamma > 7/5$ , the Mach number does not decrease through  $\mathcal{M} = 1$ . For  $R \ll 1$ , Bernoulli's equation is  $2/(\rho^2 R^6) + S\rho^{\gamma-1}/(\gamma-1) \approx \alpha/R$ . Substituting  $\rho = \eta/R^p$  with  $p = 6/(\gamma+1)$  gives  $2/\eta^2 + S\eta^{\gamma-1}/(\gamma-1) \equiv L(\eta) \approx \alpha R^{(5\gamma-7)/(\gamma-1)}$ . Clearly,  $L(\eta)$  has a minimum value of  $L_{min} = [2 + 4/(\gamma-1)](S/4)^{2/(\gamma+1)}$  at  $\eta_{min} = (4/S)^{1/(\gamma+1)}$  which corresponds to  $\mathcal{M} = 1$ . Thus for  $\gamma > 7/5$ , there is a minimum radius where a stationary flow exists,  $R_{min} = [(2/\alpha)(\gamma+1)/(\gamma-1)]^{(\gamma+1)/(5\gamma-7)}(S/4)^{2/(5\gamma-7)}$ . For most conditions this radius is expected to be less than the radius of the star.

Near the star the flow is expected to have a standing shock where  $\mathcal{M}$  discontinuously decreases to a value less than unity. For  $\gamma < 7/5$  there also must be a shock. Note that the ratio of the temperatures across this shock for an ideal gas is  $T_2/T_1 = 1 + 2(\gamma-1)(\gamma\mathcal{M}^2 + 1)(\mathcal{M}^2 - 1)/[(\gamma+1)^2\mathcal{M}^2]$  ( $\approx 2\gamma(\gamma-1)\mathcal{M}^2/(\gamma+1)^2$  for  $\mathcal{M} \gg 1$ ), where  $T_1$  is the upstream temperature and  $T_2$  is downstream (closer

to the star). Calculation of the location of this shock is beyond the scope of this work.

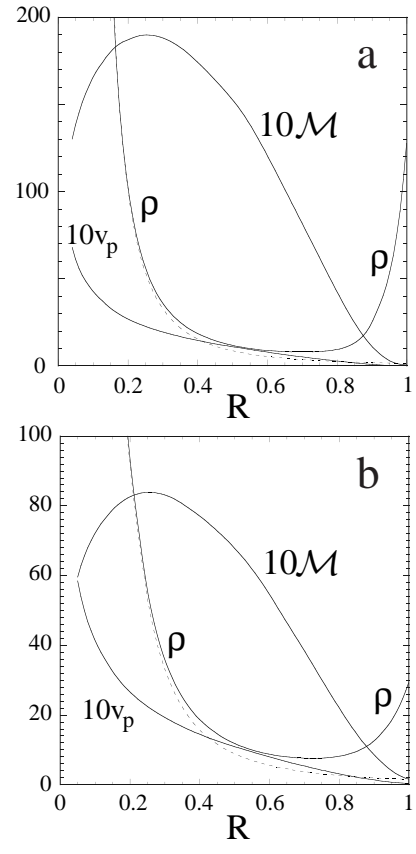


FIG. 4.— The figure shows the radial variations of the dimensionless density  $\rho$ , poloidal velocity  $v_p$ , and Mach number  $\mathcal{M} = v_p/c_s$  for cases with  $\gamma = 5/3$ ,  $\alpha = 1$ , and dimensionless entropies  $S = 0.001$  (top panel, **a**) and  $S = 0.005$  (bottom panel, **b**). For **(a)**,  $E \approx -1.462$ ,  $c_{sd} \approx 0.150$ ,  $\rho_d \approx 129.4$ ,  $R_* \approx 0.898$ , and  $c_{s*} \approx 0.0841$ . For **(b)**,  $E \approx -1.428$ ,  $c_{sd} \approx 0.218$ ,  $\rho_d \approx 29.4$ ,  $R_* \approx 0.884$ , and  $c_{s*} \approx 0.156$ . The dashed curves represent  $\text{const}R^{-5/2}$  fitted to a point at the top of the plot.

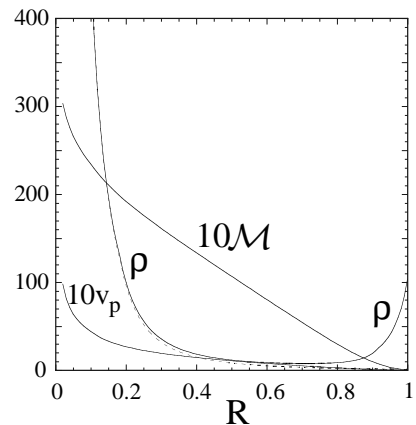


FIG. 5.— Radial variations of the dimensionless density  $\rho$ , poloidal velocity  $v_p$ , and Mach number  $\mathcal{M} = v_p/c_s$  for a case with  $\gamma = 1.3$ ,  $\alpha = 1$ , and dimensionless entropy  $S = 0.005$ . The dashed curve represents  $\text{const}R^{-5/2}$  fitted to a point at the top of the plot.

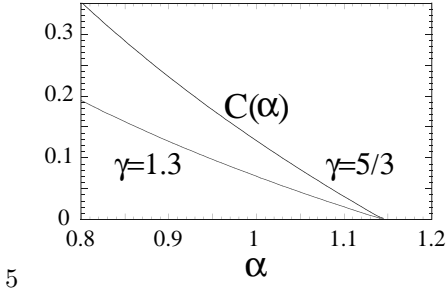


FIG. 6.— Dimensionless function in equation (20). The dimensionless sound speed  $c_{sd}$  must be less than  $C(\alpha)$ .

The value of entropy  $S$  for transonic flows  $S_{ts}$  is determined by conditions at origin of the flow at the disk where  $v_{pd}^2 \ll c_{sd}^2$ , where  $c_{sd}$  is the sound speed at the disk. At the disk,

$$E = \frac{c_{sd}^2}{\gamma - 1} - \left( \alpha + \frac{1}{2\alpha^2} \right),$$

while at the sonic point,

$$E = \frac{1}{2} \frac{\gamma + 1}{\gamma - 1} c_{s*}^2 - \left( \frac{\alpha}{R_*} + \frac{R_*^3}{2\alpha^2} \right).$$

Note that  $c_{s*}^2 = S\rho_*^{\gamma-1}$  and  $\rho_* = (4 - 3R_*)^{1/2}/(c_{s*}R_*^3)$ . Therefore, in order to have a transonic flow, we need

$$S = S_{ts} \equiv \left( \frac{2}{\gamma + 1} \right)^{\frac{\gamma+1}{2}} \left( \frac{R_*^6}{4 - 3R_*} \right)^{\frac{\gamma-1}{2}} [c_{sd}^2 - C^2(\alpha)]^{\frac{\gamma+1}{2}}, \quad (20)$$

where

$$C^2(\alpha) = (\gamma - 1) \left( \alpha + \frac{1}{2\alpha^2} - c_1\alpha^{1/4} \right)$$

is obtained by using equation (19), and  $c_1 = (3/2)^{1/4} + (2/3)^{3/4}/2 \approx 1.476$ . Figure 6 shows  $C(\alpha)$ . Clearly, for a given value of  $\alpha$  it is necessary to have sufficiently high disk temperature or disk sound speed,  $c_{sd} \geq C(\alpha)$ . This inequality and inequality (18) for transonic flow can be satisfied only for

$$\alpha_{min} \leq \alpha \leq \alpha_0, \quad (21)$$

where  $\alpha_{min}$  is such that  $c_{sd} = C(\alpha_{min})$ . Inequalities (21) correspond to a limited range of  $R_d$ ,  $r_c/\alpha_0 < R_d < r_c/\alpha_{min}$ . For example, for constant  $c_{sd} = 0.1$  and  $\gamma = 5/3$ , we have  $c_{sd} \geq C(\alpha)$  for  $1.03 \leq \alpha \leq 1.145$  and  $S$  varies between 0 and 0.00147; for  $c_{sd} = 0.2$ , the allowed range is  $0.928 \leq \alpha \leq 1.145$  and  $S$  varies between 0 and 0.00933.

## 6. SUBSONIC FLOWS

For  $\alpha_{min} \leq \alpha \leq \alpha_0$  (with  $\alpha_{min}$  given above), it is easy to show that there are outflows from the disk to the star which are subsonic. Figure 7a shows the  $R$  dependences for such a case. For  $R \ll 1$ , equation (15) gives  $c_s \approx [\alpha(\gamma - 1)/R]^{1/2}$  and  $\rho \approx [\alpha(\gamma - 1)/(SR)]^{1/(\gamma-1)}$ .

For  $\alpha < \alpha_{min}$ , there are no stationary solutions to the Bernoulli equation (15). Equivalently, there are no stationary outflows for  $R_d > r_c/\alpha_{min}$ .

For  $\alpha > \alpha_0$  or  $R_d < r_c/\alpha_0$ , there are also subsonic outflows from the disk to the star as shown in Figure 7b.

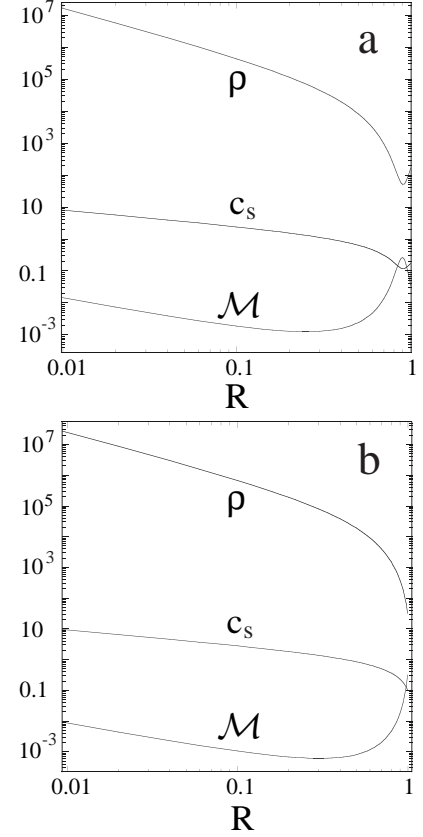


FIG. 7.— Radial dependences of density  $\rho$ , sound speed  $c_s$ , and Mach number for subsonic flows from disk to star. The top panel (a) has  $\alpha = 1.0$ ,  $S = 0.001$ ,  $\gamma = 5/3$ , and  $c_{sd} \approx 0.173$ . In this case the Mach number rises to about 0.26 at  $R = 0.9$ . The bottom panel (b) has  $\alpha = 1.3$ ,  $S = 0.001$ ,  $\gamma = 5/3$ , and  $c_{sd} \approx 0.1$ .

## 7. CONTRAST WITH BONDI ACCRETION

The Bernoulli equation(10) differs from that for spherical Bondi (1952) accretion in that here the plasma flows along the magnetic field lines, the matter is rotating, and the flow starts from a finite radius of a disk. For the Bondi flow, mass conservation gives  $4\pi R^2 \rho v_R = \dot{M} = \text{const}$  so that the Bernoulli equation is

$$E = \frac{(\dot{M}/4\pi)^2}{2\rho^2 R^4} + \frac{S\rho^{\gamma-1}}{\gamma - 1} - \frac{GM}{R}, \quad (22)$$

where  $S = c_{s\infty}^2/\rho_\infty^{\gamma-1}$ , with  $c_{s\infty}$  and  $\rho_\infty$  the sound speed and density at a large distance from the star. In contrast, the first term of equation (10) is  $\propto 1/(\rho^2 R^6)$  owing to the “focusing” of the magnetic field, and further, equation (10) includes the centrifugal potential  $-\Omega^2 r^2/2$ . For small  $R$ , the Bondi flow has  $v_R \approx (2GM/R)^{1/2}$  as in the for the up and over flow; however,  $\rho \sim 1/R^{3/2}$  and  $c_s \sim 1/R^{3(\gamma-1)/4}$ , whereas for the funnel flow  $\rho \sim 1/R^{5/2}$  and  $c_s \sim 1/R^{5(\gamma-1)/4}$ . Thus, the Mach number for the Bondi flow  $\mathcal{M} \sim 1/R^{(5-3\gamma)/4}$  always increases (or is constant) with decreasing  $R$  for  $\gamma \leq 5/3$ .

## 8. CONDITIONS FOR STRONG FIELD APPROXIMATION

In the strong field approximation of §2, the disk plasma is assumed to corotate with the star even though  $r$  is less than the corotation radius  $r_c$ . Equilibrium of this part of the disk thus requires an additional outward ra-

dial force which arises naturally from the slight bending of the field lines passing through the disk. This radial magnetic force (per unit area of the disk) is simply  $F_r^{mag} = -(B_r B_z)_h / 2\pi > 0$ , where the  $h$ -subscript indicates evaluation at the disk surface  $z = h$  [equation (5) of Lovelace *et al.* 1995]. Because  $(r_c - r)/r_c \ll 1$ , the required radial magnetic field is small,  $(B_r/B_z)_h = (6\pi\sigma\Omega^2/B_z^2)(r_c - r) = 3(\Omega r_c/v_A)^2 h(r_c - r)/r_c^2 \ll 1$ , where  $v_A$  is the Alfvén velocity based on the midplane density of the disk and  $B_z(r, 0)$ .

Also, in the approximation of §2 the toroidal magnetic field is neglected. A small deviation of the disk rotation rate  $\omega_d(r)$  from the star's rate  $\Omega$  can lead to a significant toroidal magnetic at the disk,  $(B_\phi)_h = -(hr/\eta)(\omega_d - \Omega)B_z$ , where  $\eta$  is the magnetic diffusivity of the disk [equation (2) of Lovelace *et al.* (1995)]. If  $\eta$  is of the order of the viscosity  $\nu$  given by the Shakura and Sunyaev (1973) prescription  $\nu = \alpha c_s h$  (with  $\alpha < 1$ ), then, in order to have  $|(B_\phi)_h/B_z| \ll 1$ , we must have  $|r(\omega_d - \Omega)| \ll \alpha c_s$ .

## 9. APPLICATIONS

Table 1 summarizes the relevant parameters for the cases of disk accretion to (1) a rotating magnetized neutron star, and to (2) a rotating young stellar object. In both cases, the Alfvén radius  $r_A$  (Shapiro & Teukolsky 1983) is larger than  $r_c$  so that the disk plasma is expected to corotate with the star. The disk plasma may move radially across the magnetic field by the interchange instability (Kaisig, Tajima, & Lovelace 1991; Rastätter & Schindler 1999). For the neutron star the surface magnetic field ( $\mu/R_{star}^3$ ) is assumed to be  $10^{12}$ G, while for the young star it is  $10^4$ G.

For the neutron star case, we assume  $c_{sd}/(\Omega r_c) = 0.1$  (with dimensions restored), which corresponds to a surface temperature of the disk  $T_d \approx 4.1 \times 10^7$ K for a fully ionized hydrogen plasma and  $\gamma = 1.3$  with mean particle mass  $m_H/2$ . The half-thickness of the disk is  $h \sim c_s/\Omega \approx 0.1r_c$ . From Figure 6 with  $\gamma = 1.3$ , we find that transonic outflows from the disk to the star are possible for  $\alpha$  in the range  $\alpha = r_c/R_d \approx 0.95 - 1.145$ . which corresponds to  $R_d \approx (0.873 - 1.053)r_c$ . The sonic point location  $R_*/R_d = \sin^2(\theta_*)$  has  $\theta_*$  varying between  $69^\circ$  (the lower limit of  $\alpha$  and the upper limit of  $R_d$ ) and  $90^\circ$  where the sonic point is inside the disk. The height of the sonic point  $z_* = R_d \sin^2(\theta_*) \cos(\theta_*)$  is  $\lesssim 0.273r_c$ . Thus, transonic outflows occur over an interval  $\Delta R_d \approx 0.18r_c$ . In dimensionless variables,  $\rho_d v_{pd} = 1$ . Therefore, if all of the disk accretion goes into transonic flow along the field lines,  $\dot{M}_{acc} = 2(2\pi)R_d \Delta R_d K \mu / (4\pi R_d^3)$ , where one of the factors of two in the numerator accounts for the two sides of the disk. Thus the characteristic density normalizing  $\rho$  in equation (14) is

$$\rho_0 = \frac{K\mu}{4\pi\alpha\Omega R_d^4} = \frac{\dot{M}_{acc}}{4\pi\alpha\Omega R_d^2 \Delta R_d}. \quad (23)$$

For the mentioned values and those in Table 1, we find  $\rho_0 \approx 1.4 \times 10^{-9}$ g/cm<sup>3</sup>. The ratio of the maximum to minimum radii of the flow is  $r_c/R_{star} = 150$  and that the free-fall speed at the star is  $v_{ff} = (GM/R_{star})^{1/2} \approx 1.1 \times 10^{10}$ cm/s. The angle at which the flow hits the star is  $\theta_{star} = \sin^{-1}[(R_{star}/r_c)^{1/2}] \approx 4.7^\circ$ . At this point the flow velocity is at an angle  $\approx \theta_{star}/2$  with respect to  $\hat{\mathbf{R}}$ .

For the case of a young stellar object, we assume  $c_{sd}/(\Omega r_c) = 0.05$ , which corresponds to a surface temperature of the disk  $T_d \approx 2,800$ K for a slightly ionized hydrogen plasma and  $\gamma = 5/3$ . The half-thickness of the disk is  $h \sim c_s/\Omega \approx 0.05r_c$ . The height of the sonic point is  $z_* \lesssim 0.174$ . The considerations for this case are similar to those for the neutron star. The range of  $\alpha$  is  $\approx 1.08 - 1.145$ ,  $R_d \approx (0.873 - 0.926)r_c$  and  $\Delta R_d \approx 0.053r_c$ . The angle to the sonic point varies from  $\theta_* \approx 78^\circ$  (at the lower limit of  $\alpha$ ) to  $90^\circ$ . The characteristic density in this case is  $\rho_0 \approx 10^{-12}$ g/cm<sup>3</sup>, assuming that all of the disk accretion goes into transonic flow along the field lines. The ratio  $r_c/R_{star} = 8.6$  is much smaller than for the neutron star case, and  $v_{ff}(R_{star}) \approx 365$  km/s. The angle at which the flow hits the star is  $\theta_{star} \approx 20^\circ$ . At this point the flow velocity is at an angle  $\approx 10.4^\circ$  with respect to  $\hat{\mathbf{R}}$ .

## 10. CONCLUSIONS

This work analyzes the stationary ideal magnetohydrodynamic funnel flows along the magnetic field lines of a rotating star with an aligned dipole magnetic field. Isentropic flow is assumed so that a given plasma blob maintains  $p/\rho^\gamma = \text{const}$  with  $1 < \gamma \leq 5/3$ , and the magnetic field is assumed strong,  $\rho v^2 \ll \mathbf{B}^2/4\pi$ . Earlier, Li and Wilson (1999) considered the Bernoulli equation assuming  $p \propto \rho$ . Close to the disk the flow is subsonic. There are three possible cases: (1) stationary transonic flow where a sonic point exists along the dipole field line; (2) stationary subsonic flow; and (3) no stationary flow exists. Over a range of  $R_d \lesssim r_c$ , subsonic inflows are possible, where  $R_d$  is the radius at which the dipole field line intersects the disk and  $r_c$  is the ‘corotation radius.’ For  $R_d > \sim r_c$  there are no stationary flows.

The transonic flows, which become free-fall inflow near the star, are possible only for a narrow range of  $R_d \sim r_c$ . At the sonic point these flows have an approximate balance of the centrifugal and gravitational force along the field line. The flows have different behaviors for  $\gamma > 7/5$  and  $< 7/5$ . For  $\gamma > 7/5$ , the Mach number  $\mathcal{M} \equiv |v|/c_s$  initially increases with  $R$  decreasing from  $R_d$ , but for  $R$  decreasing from  $\approx 0.22R_d$  (for  $\gamma = 5/3$ ) the Mach number decreases. In the other case,  $\gamma < 7/5$ ,  $\mathcal{M}$  increases monotonically with decreasing  $R$ . The variation of *both*  $v_p$  and  $\mathcal{M}$  are clearly important to the nature of the standing shock near the star and to the determination of emission line profiles. We discuss numerical values for funnel flows to neutron stars and young stellar objects. For the neutron star case we argue that  $\gamma$  is likely to be less than  $7/5$ . This combined with the large value of  $r_c/r_{star}$  implies that the Mach number of the flow approaching the star should be very much larger than unity. On the other hand for flows to a forming star we expect  $\gamma > 7/5$ . This combined with the not very large values of  $r_c/r_{star}$  implies only moderately large Mach numbers near the star. The flow solutions analyzed in this work are also of interest for comparison with MHD simulations.

This research was supported in part by NASA grants NAG5-9047 and NAG5-9735 and NSF grant AST-9986936. M.M.R. received partial support from NSF POWRE grant AST-9973366.

## REFERENCES

- Bondi, H. 1952, MNRAS, 112, 195  
 Camenzind, M. 1990, Rev. Mod. Astron. (Berlin: Springer), 3, 234  
 Ghosh, P., & Lamb, F.K. 1979; ApJ, 232, 259  
 Hartmann, L., Hewett, R., & Clavet, N. 1994, ApJ, 426, 669  
 Kaisig, M., Tajima, T., & Lovelace, R.V.E. 1992. ApJ, 386, 83  
 Königl, A. 1991, ApJ, 370, L39  
 Li, J., & Wilson, G. 1999, ApJ, 527, 910  
 Lovelace, R.V.E., Mehanian, C., Mobarry, C.M., & Sulkanen, M.E. 1986, ApJS, 62,1  
 Lovelace, R.V.E., Romanova, M.M., & Bisnovatyi-Kogan, G.S. 1995, MNRAS, 275, 244  
 ——— 1999, ApJ, 514, 368  
 Martin, S.C. 1996, ApJ, 470, 537  
 Najita, J.R., Edwards, S., Basri, G., & Carr, J. 2000, in *Protostars and Planets IV*, edited by V. Mannings, A.P. Boss, & S.S. Russell (Univ. of Arizona Press: Tucson), p. 457  
 Rastätter, L. & Schindler, K. 1999, ApJ, 524, 361  
 Shakura, N.I., & Sunyaev, R.A. 1973, A&A, 24, 337  
 Shapiro, S.L., & Teukolsky, S.A. 1983, *Black Holes, White Dwarfs, and Neutron Stars* (John Wiley & Sons: New York), p. 451  
 Ustyugova, G.V., Koldoba, A.V., Romanova, M.M., Chechetkin, V.M., & Lovelace, R.V.E. 1999, ApJ, 516, 221

TABLE 1  
 SAMPLE PARAMETERS<sup>a</sup>

$P$	$R_{star}$	$M$	$\dot{M}$	$L_{acc}$	$r_c$	$r_A$	$\mu$	$\Omega r_c$	$\gamma$
1 s	$10^6$ cm	$1M_{\odot}$	$10^{-9}M_{\odot}/\text{yr}$	$0.85 \times 10^{37}$ erg/s	$1.5 \times 10^8$ cm	$3.7 \times 10^8$ cm	$10^{30}$ Gcm <sup>3</sup>	$9.4 \times 10^8$ cm/s	1.3
5 d	$10^{11}$ cm	$1M_{\odot}$	$10^{-7}M_{\odot}/\text{yr}$	$0.85 \times 10^{34}$ erg/s	$8.6 \times 10^{11}$ cm	$9.6 \times 10^{11}$ cm	$10^{37}$ Gcm <sup>3</sup>	125 km/s	5/3

<sup>a</sup> $P = 2\pi/\Omega$  is the star's rotation period;  $R_{star}$  its radius;  $M$  its mass;  $\dot{M}$  is the accretion rate;  $L = GM\dot{M}/r_{star}$  is the accretion luminosity;  $r_c = (GM/\Omega^2)^{1/3}$  is the 'corotation radius';  $r_A = [\mu^4/(2GM\dot{M}^2)]^{1/7}$  is the Alfvén radius of the disk (see Shapiro and Teukolsky 1983);  $\mu$  is the magnetic moment of the star;  $\Omega r_c$  is the azimuthal velocity of the disk at the corotation radius; and  $\gamma$  is the usual adiabatic exponent.